

with increasing lithium perchlorate concentrations (Figure 8). The molar transition energy was calculated for each concentration of lithium perchlorate in both diethyl ether and tetrahydrofuran solvents so that the change in the transition energy could be monitored. This change would be indicative of the increased interactions between phenol blue and the ionic clusters in solution as the concentration of salt is increased. The molar transition energy, in kilocalories per mole, was plotted versus the log of the lithium perchlorate concentration. For diethyl ether solutions, the transition energy was linearly dependent on the log  $[\text{Li}^+, \text{ClO}_4^-]$ , with a break occurring near 4.2 M (Figure 8a) corresponding to the transition from lithium dietherate,  $\text{Li}(\text{OEt}_2)_2^+, \text{ClO}_4^-$ , to lithium monoetherate,  $\text{Li}(\text{OEt}_2)^+, \text{ClO}_4^-$  clusters.<sup>13</sup> Near this point, the slope decreased from -2.35 to -6.8. The same behavior was observed in tetrahydrofuran solution, but two breaks occurred, one at 0.3 M, with the slope decreasing from -0.49 to -4.37, and the second near 4 M, with the slope decreasing further to -12.5 (Figure 8b). This second break near 4 M, similar to the diethyl ether case, represents a transition from disolvent-coordinated lithium ion,  $\text{Li}(\text{THF})_2^+, \text{ClO}_4^-$  to the monocoordinated ion,  $\text{Li}(\text{THF})^+, \text{ClO}_4^-$ .<sup>32</sup>

The low-energy absorbance band of phenol blue continued to change with increasing salt concentration unlike the other indicators used in this study. Thus, this dye could be used as indicator of the polarity of these solutions of ionic clusters.

### Conclusion

The search for simple and useful indicators of solvent polarity continues. Here, we have presented work that shows that some indicators, which work well in pure and mixed-solvent systems,

will not behave as expected in highly ionic media, such as lithium perchlorate in diethyl ether and tetrahydrofuran. In such ionic media, the lithium ions of the media act like Lewis acids toward indicators such as Reichardt's dye, making this indicator extremely sensitive to low concentrations of lithium ion. It is possible that this indicator could be used to determine the concentration of lithium ions at the parts per million level ( $1 \times 10^{-5}$  M) in non-aqueous solutions.

On the other hand, phenol blue can detect differences in polarity of ionic systems throughout the usable concentration range of salt, up to 6 M in diethyl ether and 7 M in tetrahydrofuran. Using this dye as a polarity indicator, we discover that at above 5.0 M lithium perchlorate in diethyl ether, this ionic system is "more polar" than water.<sup>26</sup>

**Acknowledgment** is made to the donors of the Petroleum Research Fund, administered by the American Chemistry Society, for the support of this research. We also gratefully acknowledge partial support of this work by grants from the National Science Foundation and the National Institutes of Health of the U.S. Public Health Service. J.C.C. thanks the Chevron Corp. for a fellowship and the Graduate School for a scholarship.

**Registry No.** I, 2150-58-5; II, 10081-39-7; III, 120060-19-7; IV, 15310-43-7; V, 120060-20-0; VI, 120060-21-1; sodium 1,2-(dicarbomethoxy)cyclopentadienide, 68348-90-3; tropylium tetrafluoroborate, 27081-10-3; lithium, 7439-93-2; lithium perchlorate, 7791-03-9; hexane, 110-54-3; carbon tetrachloride, 56-23-5; toluene, 108-88-3; triethylamine, 121-44-8; diethyl ether, 60-29-7; chloroform, 67-66-3; ethyl acetate, 141-78-6; tetrahydrofuran, 109-99-9; methylene chloride, 75-09-2; pyridine, 110-86-1; isopropyl alcohol, 67-63-0; acetone, 67-64-1; ethanol, 64-17-5; methanol, 67-56-1; dimethylformamide, 68-12-2; acetonitrile, 75-05-8; ethylene glycol, 107-21-1; dimethyl sulfoxide, 67-68-5; water, 7732-18-5; *N*-methylacetamide, 79-16-3.

(32) Pocker, Y.; Ciula, J. C., unpublished results.

## Affinities of Racemic and Meso Forms of *N,N'*-Ethylenebis[2-(*o*-hydroxyphenyl)glycine] for Divalent and Trivalent Metal Ions

Christopher J. Bannochie and Arthur E. Martell\*

Contribution from the Department of Chemistry, Texas A&M University, College Station, Texas 77843. Received August 17, 1988

**Abstract:** The commercially available multidentate ligand *N,N'*-ethylenebis[2-(*o*-hydroxyphenyl)glycine] (EHPG) contains a mixture of racemic and meso forms of the ligand. Theoretical work has addressed the differences in the stabilities of the meso and racemic isomers, which until the current study have not been measured. In this study the commercial ligand has been separated into a racemic mixture and meso isomer, and potentiometric and spectrophotometric stability measurements have been made of each. Reported here for both forms at 25.0 °C and  $\mu = 0.10$  M (KCl) are ligand protonation constants as well as chelate protonation, stability, and hydrolysis constants with the divalent metal ions Ni(II), Cu(II), and Zn(II) and the trivalent metal ions Fe(III), Ga(III), and In(III). In all cases *rac*-EHPG forms the more stable complexes. Since the basicities of the two ligands are essentially the same (*rac*-EHPG, 38.0; *meso*-EHPG, 37.9), these ligands provide an interesting example whereby the differences observed in the stabilities of their complexes are due to differences in coordination geometry. A comparison of the equilibrium distribution of metal ion between each form of EHPG and the iron transport protein transferrin indicates that while the racemic and meso forms of the ligand may compete successfully in vivo for Fe(III) and Ga(III), the In(III) complexes are decidedly weaker and may be converted completely to the transferrin complexes, provided that the exchange kinetics are sufficiently rapid.

Interest in the multidentate ligand *N,N'*-ethylenebis[2-(*o*-hydroxyphenyl)glycine] (EHPG) has been long and varied. Initially this interest focused on the ability of its extremely stable iron chelate to alleviate iron chlorosis in plants caused by alkaline soil conditions.<sup>1</sup> Much later EHPG was used as an active site

model of the iron transport protein transferrin.<sup>2-7</sup> Most recently work has focused on the unique vanadium coordination chemistry

(2) Gaber, B. P.; Miskowski, V.; Spiro, T. G. *J. Am. Chem. Soc.* **1974**, *96*, 6868.

(3) Chasteen, N. D. *Coord. Chem. Rev.* **1977**, *22*, 1.

(4) Pecoraro, V. L.; Harris, W. R.; Carrano, C. J.; Raymond, K. N. *Biochemistry* **1981**, *20*, 7033.

(1) Kröll, H.; Knell, M.; Powers, J.; Simonian, J. *J. Am. Chem. Soc.* **1957**, *79*, 2024.

demonstrated by EHPG.<sup>8-12</sup> Our interest in the affinities of the racemic and meso forms of EHPG has been 2-fold. First, until the present study, the presence of these two forms of EHPG have not been systematically considered in the determination of metal complex stability. Additionally, EHPG is of interest to us as a potential radiopharmaceutical carrier in positron emission tomography; the iron(III) chelate is also of interest as a paramagnetic contrast agent for magnetic resonance imaging.<sup>13</sup>

Though the separation of the racemic mixture and meso isomer was first reported by Ryskiewich and Boka<sup>14</sup> in 1962, early investigations into the equilibrium behavior of EHPG did not consider the presence of isomers resulting from the two chiral centers.<sup>15-23</sup> By not addressing the isomers, which have since been shown to be present in approximately 1:1 ratio,<sup>5</sup> these stability determinations dealt with systems that contained a mixture of two different compounds. In this study the commercially available ligand has been separated into a racemic mixture and meso isomer. Ligand protonation constants as well as chelate protonation, stability, and hydrolysis constants with the divalent metal ions Ni(II), Cu(II), and Zn(II) and the trivalent metal ions Fe(III), Ga(III), and In(III) are reported. The stability constants have been determined by potentiometric back-titration and spectrophotometric titration.

### Experimental Section

**Materials.** EHPG was obtained from Dojindo Labs (Japan) under the alternate name ethylenediamine-*N,N'*-bis[ $\alpha$ -(2-hydroxyphenylacetic acid)] (EDDHA). Reagent-grade nickel(II) chloride, copper(II) chloride, zinc(II) chloride, and iron(III) chloride were obtained from Fisher Scientific Co. and used without further purification. Gallium(III) chloride and indium(III) chloride were obtained from Aldrich Chemical Co. and E. H. Sargent & Co., respectively. Carbonate-free ampules of Dilut-It KOH were obtained from J. T. Baker Chemical Co. All aqueous solutions were prepared with CO<sub>2</sub>-free, doubly distilled water. After dilution, the KOH solution was standardized by titration of potassium hydrogen phthalate to a phenolphthalein endpoint. This standard KOH titrant was then used to standardize an aqueous solution of HCl. Solutions of Ga(III) and In(III) were standardized by ion exchange using Dowex 50W-X8 cation-exchange resin (20-50 mesh), followed by titration of the free acid liberated. All the remaining metal ion solutions were standardized according to the methods of Schwarzenbach and Flaschka.<sup>24</sup>

**rac-EHPG.** The racemic mixture was obtained in pure form from the commercially available ligand through isolation of crystals of Mg[Fe(*rac*-EHPG)]<sub>2</sub> as described by Bailey et al.<sup>25</sup> The metal-free ligand was

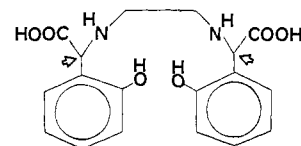


Figure 1. Structure of *N,N'*-ethylenebis[2-(*o*-hydroxyphenyl)glycine] (EHPG). Arrows indicate chiral carbon centers.

obtained by removal of Fe(III) from the complex by precipitation of Fe(OH)<sub>3</sub> using 3 M KOH under an inert atmosphere of N<sub>2</sub>, to prevent oxidation of the ligand and vacuum filtration of the basic solution through acid-washed Celite. Acidification of the basic supernatant liquid with 6 M HNO<sub>3</sub> to p[H] 4-5 resulted in precipitation of the ligand.

**meso-EHPG.** The meso isomer was obtained by employing "dry-column" chromatography<sup>26</sup> to simulate the TLC separation of the racemic and meso iron complexes by the use of a mobile phase containing 10:2:1 *n*-butanol/water/acetic acid, respectively. The column stationary phase consisted of Baker No. 3405 (60-200 mesh) silica gel, which had been checked for deactivation to activity III as described by Loev and Goodman<sup>26</sup> and equilibrated for 2 h with 10% mobile phase on a lathe. A glass column (108 × 5 cm) fitted with a sintered glass frit was packed with 1200 g of equilibrated silica gel. The 5 g of iron chelate solution remaining from crystallization of Mg[Fe(*rac*-EHPG)]<sub>2</sub> was rotary evaporated, dispersed on 25 g of silica gel, and loaded onto the column after having been dried in a vacuum desiccator. The column was eluted with mobile phase for 15 h until the lead violet-colored band of the meso chelate reached the glass frit. Column development was then stopped and the violet band separated from the trailing red-brown band of the racemic ligand complex. After this band was air-dried, the iron(III) complex was eluted from the silica gel with methanol and rotary evaporated, and the iron-free meso ligand was obtained as described above for the racemic ligand.

Another method for obtaining the meso isomer, which does not employ chromatography, has been described,<sup>6</sup> but in our hands it did not satisfactorily yield the pure isomer.

The racemic mixture and meso isomer were identified by TLC of their iron complexes on silica gel 60 precoated sheets by use of the mobile phase described above (racemic complex *R<sub>f</sub>* = 0.29, meso complex *R<sub>f</sub>* = 0.33) and by NMR<sup>11</sup> of the metal-free ligand.

**Potentiometric Equilibrium Determinations.** A Corning Model 150 pH-Ion meter fitted with Corning glass and calomel reference electrodes was used in the determination of hydrogen ion concentration in all potentiometric measurements. Measurements were made at 25.00 ± 0.05 °C in a sealed, water-jacked glass vessel, which was maintained under an inert atmosphere of purified, 0.100 M KCl saturated N<sub>2</sub>. Standard aqueous HCl and KOH solutions were used to calibrate the electrodes and meter to read -log [H<sup>+</sup>] directly. In this paper -log [H<sup>+</sup>] is designated as p[H]. A Gran's plot<sup>27</sup> analysis was used to check for carbonate contamination of the standard aqueous KOH and consistently revealed less than 0.5% carbonate. Ionic strength was maintained at 0.100 M with reagent-grade KCl.

Due to the insolubility of both forms of EHPG below p[H] 5 at the concentrations used in the potentiometric measurements (see below), all data were obtained by back-titration with aqueous 0.1000 M HCl titrant. Solutions of EHPG were prepared under N<sub>2</sub> with 2 equiv of base prior to each experiment. After mixing, the experimental solution was raised to between p[H] 10-11.5, depending upon the system under investigation, with standard aqueous 0.1000 M KOH and then back-titrated to p[H] 2 or until precipitation of ligand occurred. The concentration of ligand, as well as metal ion in [1:1] ligand:metal experiments, was 2.00 × 10<sup>-3</sup> M for the experiments with the racemic mixture and 1.00 × 10<sup>-3</sup> M for those employing the meso isomer (the lower concentration necessitated by sample size limitations).

The third and fourth ligand protonation constants as well as chelate protonation, stability, and hydrolysis constants for the [1:1] metal:ligand systems were calculated by the use of the FORTRAN program BEST.<sup>28</sup> The method used in the computations are those which have been described in detail elsewhere.<sup>29</sup> Species distribution diagrams were calculated with the FORTRAN program SPE<sup>29</sup> written in this laboratory.

(5) Patch, M. G.; Simolo, K. P.; Carrano, C. J. *Inorg. Chem.* **1982**, *21*, 2972.

(6) Patch, M. G.; Simolo, K. P.; Carrano, C. J. *Inorg. Chem.* **1983**, *22*, 2630.

(7) Riley, P. E.; Pecoraro, V. L.; Carrano, C. J.; Raymond, K. N. *Inorg. Chem.* **1983**, *22*, 3096.

(8) Pecoraro, V. L.; Bonadies, J. A.; Marrese, C. A.; Carrano, C. J. *J. Am. Chem. Soc.* **1984**, *106*, 3360.

(9) Carrano, C. J.; Spartialian, K.; Appa Rao, G. V. N.; Pecoraro, V. L.; Sundaralingam, M. *J. Am. Chem. Soc.* **1985**, *107*, 1651.

(10) Riley, E. P.; Pecoraro, V. L.; Carrano, C. J.; Bonadies, J. A.; Raymond, K. N. *Inorg. Chem.* **1986**, *25*, 154.

(11) Bonadies, J. A.; Carrano, C. J. *J. Am. Chem. Soc.* **1986**, *108*, 4088.

(12) Bonadies, J. A.; Carrano, C. J. *Inorg. Chem.* **1986**, *25*, 4358.

(13) Lauffer, R. B.; Vincent, A. C.; Padmanabhan, S.; Meade, T. J. *J. Am. Chem. Soc.* **1987**, *109*, 2216.

(14) Ryskiewich, D. P.; Boka, G. *Nature* **1962**, 193.

(15) Frost, A. E.; Freedman, H. H.; Westerbach, S. J.; Martell, A. E. *J. Am. Chem. Soc.* **1958**, *80*, 530.

(16) Schroder, K. H. *Nature* **1964**, *202*, 898.

(17) Schroder, K. H. *Acta Chem. Scand.* **1964**, *3*, 596.

(18) Anderegg, G.; L'Eplattenier, F. *Helv. Chim. Acta* **1964**, *47*, 1067.

(19) Nozaki, T.; Ohno, Y. *Nippon Kagaku Kaishi* **1973**, 1455.

(20) Harris, W. R.; Martell, A. E. *Inorg. Chem.* **1976**, *15*, 713.

(21) Salama, S.; Richardson, F. S. *Inorg. Chem.* **1980**, *19*, 635.

(22) Rajan, K. S.; Mainer, S.; Rajan, N. L.; Davis, J. M. *J. Inorg. Biochem.* **1981**, *14*, 339.

(23) Taliaferro, C. H.; Motekaitis, R. J.; Martell, A. E. *Inorg. Chem.* **1984**, *23*, 1188.

(24) Schwarzenbach, G.; Flaschka, H. *Complexometric Titrations*; Methuen: London, 1969.

(25) Bailey, N. A.; Cummins, D.; McKenzie, E. D.; Worthington, J. M. *Inorg. Chem. Acta* **1981**, *50*, 111.

(26) Loev, B.; Goodman, M. M. *Progress in Separations and Purifications*; Interscience: New York, 1970; Vol. III, p 73.

(27) Rossotti, F. J. C.; Rossotti, H. *J. Chem. Educ.* **1965**, *42*, 375.

(28) Motekaitis, R. J.; Martell, A. E. *Can. J. Chem.* **1982**, *60*, 2403.

(29) Motekaitis, R. J.; Martell, A. E. *Determination and Use of Stability Constants*; VCH Publishers: New York, 1989.

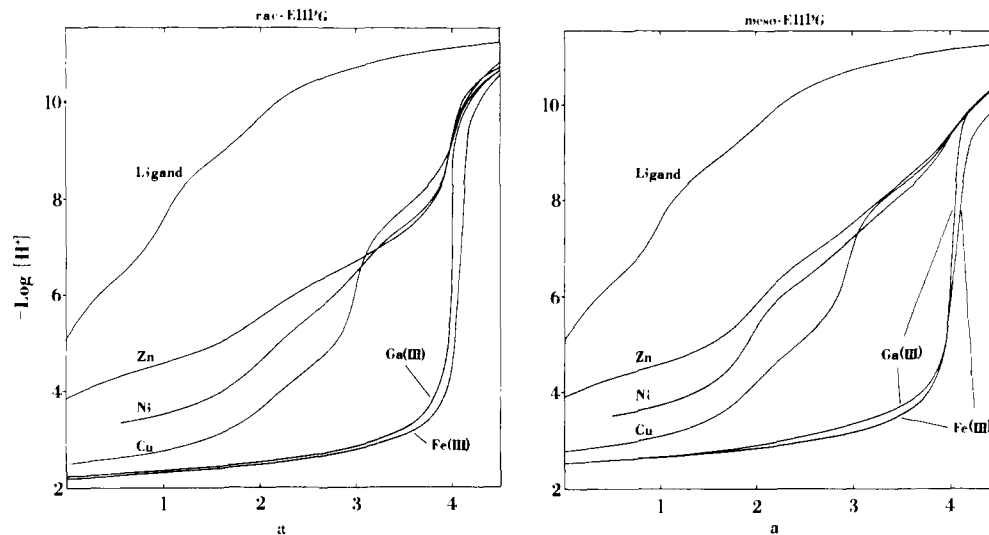


**Figure 2.** Potentiometric equilibrium curves for *rac*- and *meso*-EHPG [*N,N'*-ethylenebis[2-(*o*-hydroxyphenyl)glycine] obtained by back-titration. Initial concentrations for *rac*-EHPG experiments: ligand alone  $1.83 \times 10^{-3}$  M;  $[\text{Zn}^{2+}]_{\text{tot}} = 1.63 \times 10^{-3}$  M and  $[\text{L}]_{\text{tot}} = 1.64 \times 10^{-3}$  M;  $[\text{Ni}^{2+}]_{\text{tot}} = 1.59 \times 10^{-3}$  M and  $[\text{L}]_{\text{tot}} = 1.60 \times 10^{-3}$  M;  $[\text{Cu}^{2+}]_{\text{tot}} = 1.92 \times 10^{-3}$  M and  $[\text{L}]_{\text{tot}} = 1.92 \times 10^{-3}$  M;  $[\text{Ga}^{3+}]_{\text{tot}} = 1.93 \times 10^{-3}$  M and  $[\text{L}]_{\text{tot}} = 1.94 \times 10^{-3}$  M;  $[\text{Fe}^{3+}]_{\text{tot}} = 1.87 \times 10^{-3}$  M and  $[\text{L}]_{\text{tot}} = 1.87 \times 10^{-3}$  M. Initial concentrations for *meso*-EHPG experiments: ligand alone  $1.94 \times 10^{-3}$  M;  $[\text{Zn}^{2+}]_{\text{tot}} = 9.91 \times 10^{-4}$  M and  $[\text{L}]_{\text{tot}} = 9.94 \times 10^{-4}$  M;  $[\text{Ni}^{2+}]_{\text{tot}} = 9.72 \times 10^{-4}$  M and  $[\text{L}]_{\text{tot}} = 9.73 \times 10^{-4}$  M;  $[\text{Cu}^{2+}]_{\text{tot}} = 9.46 \times 10^{-4}$  M and  $[\text{L}]_{\text{tot}} = 9.49 \times 10^{-4}$  M;  $[\text{Ga}^{3+}]_{\text{tot}} = 1.03 \times 10^{-3}$  M and  $[\text{L}]_{\text{tot}} = 1.04 \times 10^{-3}$  M;  $[\text{Fe}^{3+}]_{\text{tot}} = 9.66 \times 10^{-4}$  and  $[\text{L}]_{\text{tot}} = 9.68 \times 10^{-4}$  M. Temperature, 25.0 °C;  $\mu = 0.10$  M (KCl); *a* is the moles of standard KOH solution added per mole of ligand present.

**Spectrophotometric Equilibrium Measurements.** The optical absorption spectra of the ligand and metal complex species were measured with a Perkin-Elmer Model 553 fast-scan spectrophotometer and universally matched quartz cells of path length  $1.000 \pm 0.001$  cm. Solutions were  $1.00 \times 10^{-4}$  M in ligand or ligand and metal. Ionic strength was maintained at 0.100 M with KCl. Successive spectra were obtained by the addition of standard aqueous 0.1000 M HCl or KOH. Dilution was accounted for in the calculations. Extinction coefficients and protonation constants for the phenolic protons were determined from the ultraviolet absorption band arising at 295 nm as a result of the phenolate chromophore by using the FORTRAN program ABSPKAS (extinction coefficients and/or log protonation constants can be adjusted to give the best agreement between calculated and observed absorbance for each spectrum) written in this laboratory.

Stability constants for the iron(III) complexes of *rac*- and *meso*-EHPG were calculated from the absorption bands arising at 485 and 480 nm, respectively, by using the BASIC program KML. Ligand protonation and chelate protonation constants were determined potentiometrically and spectrophotometrically in separate experiments as previously described above. The extinction coefficients for the iron complex of each ligand were determined from the maximum observed absorbance and supplied to the program along with the absorbance, measured p[H], and volume parameters for each spectrum. The program calculates a  $\log K_{\text{ML}}$  for each absorbance and then recalculates the absorbance, percent free metal ion and percent complex at each experimental point from the average  $\log K_{\text{ML}}$ . In the case of *meso*-EHPG the extinction coefficient for the protonated metal chelate was unknown and was therefore varied to give the best agreement between the observed and calculated absorbances. Data taken in the range between where there was at least 10% free metal and 10% metal complex were used in the final calculation of  $\log K_{\text{ML}}$ .

**Results and Discussion**

**Isomer Separation.** A racemic mixture of the multidentate ligand EHPG (Figure 1) arises when the two chiral centers have the same absolute configurations, either (*R,R*) or (*S,S*). The crystallization of  $\text{Mg}[\text{Fe}(\text{rac-EHPG})]_2$  as described by Bailey et al.<sup>25</sup> provides an elegant and convenient method for obtaining the racemic mixture without traces of the meso isomer, absolute configuration (*R,S*). Ryskiewicz and Boka reported<sup>14</sup> that two forms of the iron complex could be separated and visualized with TLC by use of the upper layer of a 4:1:5 mixture of *n*-butanol/acetic acid/water. Reported here is a more conveniently prepared and reliable mobile phase consisting of a 10:2:1 mixture of *n*-butanol/water/acetic acid. Since the iron complexes of the racemic mixture and meso isomer can readily be observed as red-brown ( $R_f = 0.29$ ) and violet ( $R_f = 0.33$ ) spots, respectively, in TLC this seemed a logical way to obtain the meso isomer in

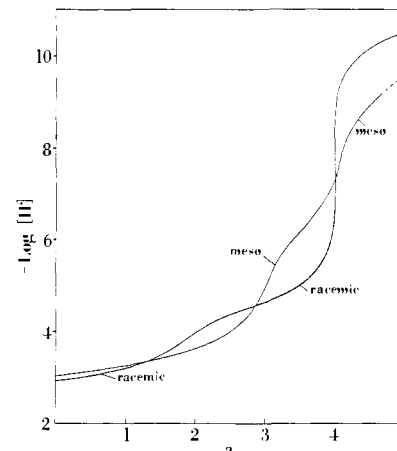


**Figure 3.** Potentiometric equilibrium curves for In(III) EHPG [1:1]. Initial concentrations:  $[\text{rac-EHPG}]_{\text{tot}} = 9.81 \times 10^{-4}$  M and  $[\text{In}^{3+}]_{\text{tot}} = 9.78 \times 10^{-4}$  M;  $[\text{meso-EHPG}]_{\text{tot}} = 9.84 \times 10^{-4}$  M and  $[\text{In}^{3+}]_{\text{tot}} = 9.78 \times 10^{-4}$  M. Temperature, 25.0 °C;  $\mu = 0.10$  M (KCl); *a* is the moles of standard KOH solution added per mole of ligand present.

**Table I.** Log Protonation Constants for *rac*- and *meso*-EHPG<sup>a</sup>

const	equilbrm	<i>rac</i> -EHPG	<i>meso</i> -EHPG
$K_1^{\text{H}}$	HL/H·L	12.05	11.90
$K_2^{\text{H}}$	H <sub>2</sub> L/H·HL	10.87	10.85
$K_3^{\text{H}}$	H <sub>3</sub> L/H·H <sub>2</sub> L	8.79	8.76
$K_4^{\text{H}}$	H <sub>4</sub> L/H·H <sub>3</sub> L	6.33	6.36

<sup>a</sup> Values obtained at  $\mu = 0.10$  M (KCl), 25.0 °C.

pure form. Dry-column chromatography<sup>26</sup> provides a convenient method of extrapolating TLC separations to preparative-scale separations, and it is this method that was used to obtain the iron complex of *meso*-EHPG without traces of the complex of the racemic mixture.

**Thermodynamic Stabilities.** Potentiometric equilibrium curves are shown in Figures 2 and 3 for the racemic mixture and meso isomer of EHPG and their [1:1] metal:ligand p[H] profiles with Ni(II), Cu(II), Zn(II), Fe(III), Ga(III), and In(III). These data were analyzed with the FORTRAN program BEST<sup>28</sup> written in this laboratory. Protonation and stability constants were varied to achieve the best possible fit between the observed and calculated p[H] at each datum point according to the stoichiometric pa-

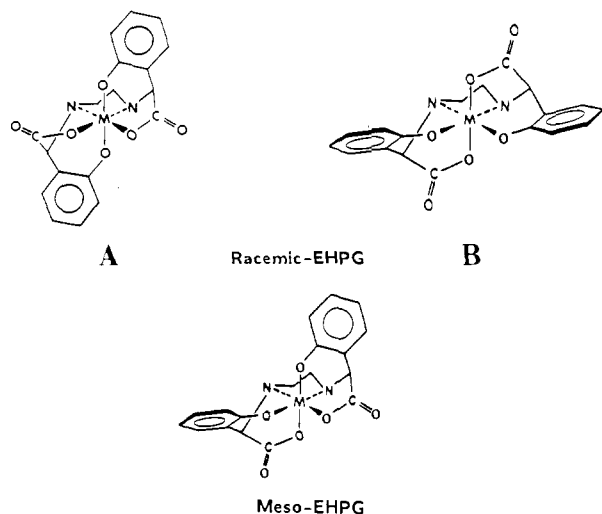


**Figure 4.** Coordination geometries of *rac*- and *meso*-EHPG when serving as a hexacoordinate ligand to a generalized octahedrally coordinated metal ion. (A) Phenolate oxygens in axial positions of plane defined by ethylenediamine ring for *rac*-EHPG. (B) Carboxylate oxygens in axial positions of plane defined by ethylenediamine ring for *rac*-EHPG.

rameters supplied. Table I lists the protonation constants determined for each ligand. The first two protonations,  $K_1^H$  and  $K_2^H$ , correspond to phenolate oxygen protonations and were determined spectrophotometrically from the ultraviolet absorption band arising at 295 nm. It is necessary, particularly in the case of  $K_1^H$ , to turn to spectrophotometry because the protonation constant of about 12 log units in each case is at the limit of the potentiometric method.<sup>29</sup> Log  $K_3^H$  and  $K_4^H$  were determined by potentiometric back-titration and correspond to the protonation constants of the secondary amine nitrogens. It is not possible to obtain the protonation constants corresponding to the carboxylate oxygens because after addition of the fourth equivalent of acid in the back-titration one observes precipitation of each ligand from solution as the zwitterionic form is lost. A similar precipitation occurs in the Ni(II) experiments, resulting in separation of the uncomplexed ligand from solution and the incomplete p[H] profile observed in Figure 2.

It is of particular interest to note that the basicities of the two ligands are the same within experimental uncertainty (*rac*-EHPG, 38.0; *meso*-EHPG, 37.9), the basicity being determined by the sum of the log protonation constants. Since two of the major factors leading to metal complex stability are ligand basicity and favorable coordination geometry, these ligands provide an interesting example whereby the differences observed in the stabilities of their complexes are almost entirely due to differences in coordination geometry.

Theoretical work has addressed the differences in the stabilities of the racemic mixture and meso isomer which until this study have not been measured.<sup>30</sup> Shown in Figure 4 are the chelate structures possible for the two compounds when serving as hexacoordinate ligands to a metal ion. Greater stability has been proposed for structure B due to the geometric selectivity in the placement of both six-membered chelate rings, with their greater bite angle, in the equatorial plane defined by the ethylenediamine ring.<sup>30</sup> On the basis of this argument, arrangement A should be the least likely form. This has been supported in the solid state by the absence of any observed structure A in the crystal structures that have been performed of Fe(III),<sup>26</sup> Co(III), Cu(II), and Ga(III)<sup>7</sup> racemic EHPG complexes. In the case of the meso isomer the only arrangement possible is the one with all like coordinating groups cis to one another. This structure, shown in Figure 4, is intermediate between the highly strained arrangement A and most favorable arrangement B of the racemic mixture. It should be noted that each of the diastereomers shown in Figure 4 is one member of an enantiomeric pair resulting from the ab-

**Table II.** Log Stability Constants of Divalent Metal Ions with *rac*- and *meso*-EHPG<sup>a</sup>

metal ion	equilbrm	<i>rac</i> -EHPG	<i>meso</i> -EHPG
Ni <sup>2+</sup>	ML/M·L	21.33	19.42
Cu <sup>2+</sup>	ML/M·L	25.27	23.68
Zn <sup>2+</sup>	ML/M·L	18.66	16.88

<sup>a</sup> Values obtained at  $\mu = 0.10$  M (KCl), 25.0 °C.

**Table III.** Differences in Log K Values for *rac*- and *meso*-EHPG

metal ion	ML/M·L	MHL/H·ML	MH <sub>2</sub> L/H·MHL
Ni <sup>2+</sup>	1.91	-0.69	-0.91
Cu <sup>2+</sup>	1.59	-0.55	-0.70
Zn <sup>2+</sup>	1.78	-1.14	-0.65
In <sup>3+</sup>	1.42	-1.67	1.36

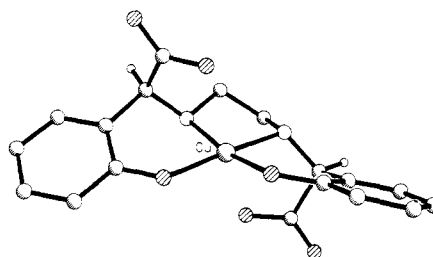


**Figure 5.** Suggested coordination geometry for Cu(*rac*-EHPG).

solute configuration of the complex. No difference in stability would be expected between the members of each diastereomeric pair.

Table II presents the stability constants of the divalent metal ions Ni(II), Cu(II), and Zn(II) with both *rac*- and *meso*-EHPG. The relative stabilities of these complexes were evident in the degree of successively lower displacement of the [1:1] metal:ligand curves from that of the free ligand in Figure 2. In all cases the racemic ligand forms the more stable complexes. The decreased stability for the *meso*-EHPG complexes is just over 1.9 log units in the case of Ni(II) and nearly 1.6 and 1.8 log units for Cu(II) and Zn(II), respectively as shown in Table III. A recent crystal structure of Na<sub>2</sub>[Cu(*rac*-EHPG)]·5.5H<sub>2</sub>O by Raymond et al.<sup>7</sup> led the authors to suggest that the stability difference between the *rac*- and *meso*-EHPG complexes of Cu(II) should be even greater than that observed in the Fe(III) complexes (nearly 2.3 log units, see Table V) due to the large tetragonal distortion evident in its complexes, i.e., the Cu(II) *meso*-EHPG complex would be additionally destabilized by the placement of a phenol substituent in an elongated axial position. At least in this work that type of behavior does not appear to be the case. In fact the Cu(II) complexes show the smallest difference in stability of the divalent metal ions studied. It is likely that in solution the ML species for the Cu(II) complexes of each ligand have the approximately square-planar configuration proposed by Frost et al.<sup>15</sup> and shown for *rac*-EHPG in Figure 5. In the case of the [Cu(*meso*-EHPG)]<sup>2-</sup> complex, space-filling molecular models reveal that the coordination of both phenolate oxygens in the plane defined by the ethylenediamine chelate ring would place both carboxylate donor groups on the same side of the molecule. As described by Frost et al.,<sup>15</sup> the successive protonations of the copper complexes would result in two rearrangements as the phenolate oxygen donor groups are replaced by carboxylate oxygen donor groups in the coordination sphere. It has been shown by these authors that in the absence of the carboxylate groups, as in the compound *N,N'*-bis(2-hydroxybenzyl)ethylenediamine, stepwise formation of the final complex does not occur. Hence the behavior observed for both forms of EHPG is a result of the formation of stable protonated intermediate complexes.

Each of the divalent metal complexes of *rac*- and *meso*-EHPG shows (Figure 2) the formation of protonated metal chelate species at  $a$  values of 2.5 and 3.5 (where  $a$  is the ratio of the moles of base added to the moles of ligand present). These protonated chelate species, MHL<sup>-</sup> and MH<sub>2</sub>L, correspond to protonation of

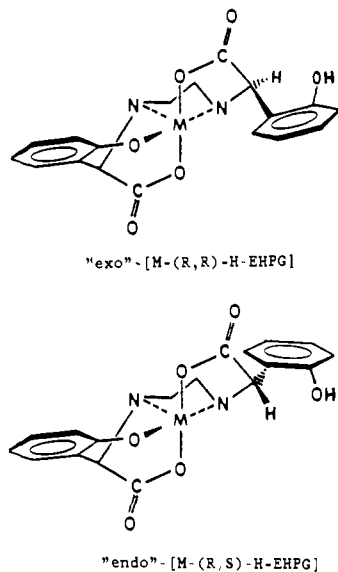
(30) Bernauer, K. *Top. Curr. Chem.* 1976, 65, 1.

Table IV. Comparison of EHPG Chelate Protonation Constants

metal ion	equilbrm	<i>rac</i> -EHPG <sup>a</sup>	mixture EHPG <sup>b</sup>	<i>meso</i> -EHPG <sup>a</sup>
Ni <sup>2+</sup>	MHL/H·ML	7.42	7.63	8.11
	MH <sub>2</sub> L/H·MHL	5.50	6.03	6.41
Cu <sup>2+</sup>	MHL/H·ML	7.82	8.04	8.37
	MH <sub>2</sub> L/H·MHL	4.44	4.98	5.14
Zn <sup>2+</sup>	MHL/H·ML	7.14	7.74	8.28
	MH <sub>2</sub> L/H·MHL	6.18	6.64	6.83

<sup>a</sup> Values obtained at  $\mu = 0.10$  M (KCl), 25.0 °C. <sup>b</sup> Values obtained from ref 15.

Chart I



the phenolate oxygen atoms of each ligand, and the values found for these equilibria are given in Table IV. In each case the protonation constants for the *meso* isomer chelates are higher, i.e., protonation of the metal chelate occurs at higher p[H] values, than those of the racemic ligand complexes. This behavior is expected if one considers that the coordination pattern is fixed only in the case of the ML complex. It has been noted that, upon formation of the protonated species MHL<sup>-</sup> and MH<sub>2</sub>L, both forms of EHPG allow the same coordination arrangement. In the case of MHL<sup>-</sup>, the only difference between the racemic and *meso* forms is a result of the chirality of the  $\alpha$ -carbon atom containing the protonated phenol and hence the relative position of this uncoordinated donor site. For the racemic mixture this position is *exo* while for the *meso* ligand it is *endo* (Chart I). The *exo* or *endo* position of the free phenolic group is fixed by closure of the first phenolate chelate ring. Since the *exo* position of a substituent has been found to be favored for similar pentacoordinate compounds, this may account for the greater selectivity, larger difference between the diastereomers, observed for closure of the first phenolate ring around Ni(II) and Cu(II) (see Table III). In the case of Zn(II) and In(III) the selectivity pattern is reversed. If an analogy is drawn between the molecular framework and coordination pattern of EHPG and that of two histidine molecules, one may account for the reversal noted through the observation that Zn(His)<sub>2</sub> has a strongly distorted octahedral geometry, with the four nitrogen donor atoms forming an almost tetrahedral arrangement, while Ni(His)<sub>2</sub> has a regular octahedral structure.<sup>31</sup> In Zn(EHPG) the two carboxylate donor groups may be only weakly interacting with the metal ion.

Also shown in Table IV are the previously published chelate protonation constants determined by Frost et al.<sup>15</sup> for an unspecified mixture (but probably ~50-50) of the racemic and *meso* forms of EHPG. It is interesting how closely these previously determined values lie to the mean of the *rac*- and *meso*-EHPG

Table V. Log Stability Constants of Trivalent Metal Ions with *rac*- and *meso*-EHPG<sup>a</sup>

metal ion	equilbrm	<i>rac</i> -EHPG	<i>meso</i> -EHPG
Fe <sup>3+</sup>	ML/M·L	35.54	33.28
	MHL/H·ML		2.72
	ML/H·MOHL	11.78	10.45
Ga <sup>3+</sup>	ML/M·L	33.89	32.40
	MHL/H·ML	2.22	3.44
In <sup>3+</sup>	ML/M·L	26.68	25.26
	MHL/H·ML	4.47	6.14
	MH <sub>2</sub> L/H·MHL	4.78	3.42
	ML/H·MOHL	10.57	8.83

<sup>a</sup> Values obtained at  $\mu = 0.10$  M (KCl), 25.0 °C.

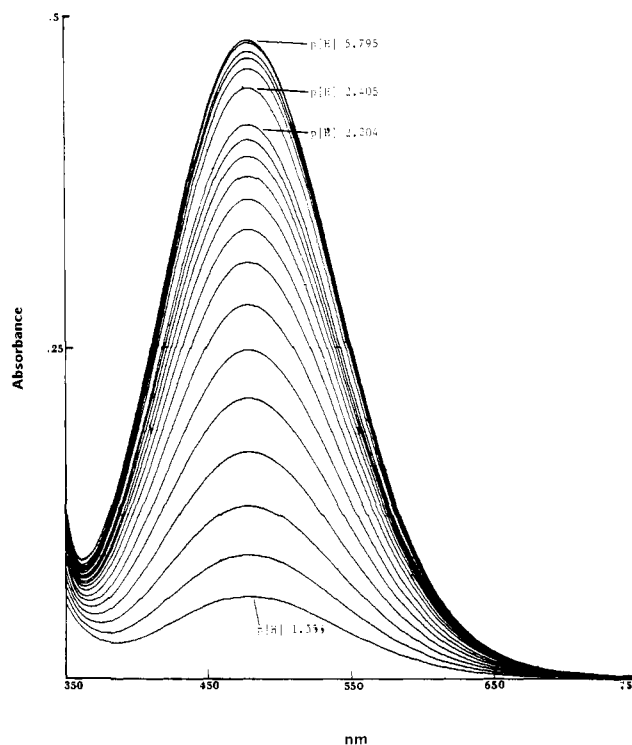
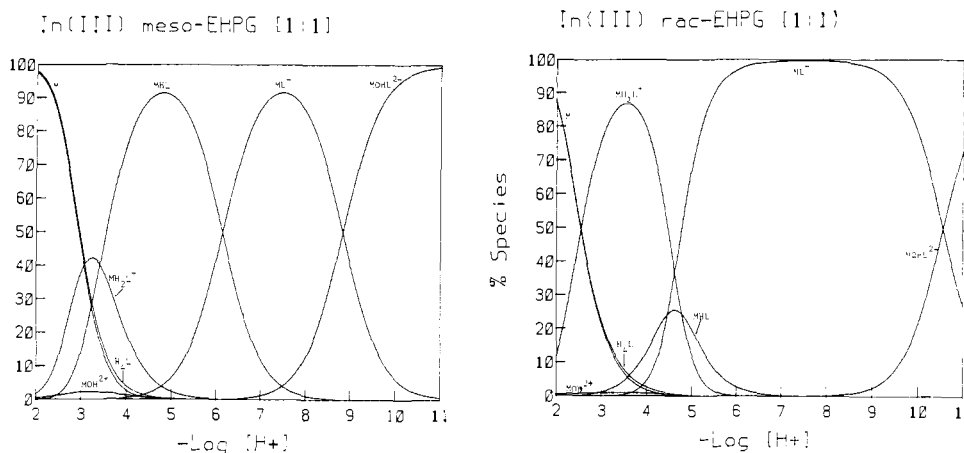


Figure 6. Effect of p[H] on the optical spectrum of Fe(*rac*-EHPG). Initial concentrations: Fe(III),  $9.90 \times 10^{-5}$  M; *rac*-EHPG,  $9.91 \times 10^{-5}$  M. Spectra are shown uncorrected for dilution. Temperature, 25.0 °C;  $\mu = 0.10$  M (KCl). p[H] increment is 0.05 from p[H] 1.553 to 2.204.

values. In effect what was done in the previous work was to fit the overlapping buffer regions of these two ligands to one constant. Prior to the use of modern computing techniques this was an understandable error, but it does point out one important point. When fitting experimental data it is extremely important to supply all possible species to the model (being ever mindful to avoid overspeciation) in order to avoid neglecting real species that may be present.

Both *rac*- and *meso*-EHPG have high affinities for trivalent metal ions (Table V). As hard acids, trivalent metal ions are strongly attracted to the two phenolate donor groups (hard bases) on each of these ligands. In the case of [Fe(*rac*-EHPG)]<sup>-</sup>, which is better than 95% formed at p[H] 2, it is necessary to turn to spectrophotometry and very low p[H]s to accurately determine the stability constant. Shown in Figure 6 is the optical absorption spectra for the L → M charge-transfer band of [Fe(*rac*-EHPG)]<sup>-</sup> measured between p[H] 1.55 and 5.80. From the observed absorbance, measured p[H], and extinction coefficient of 4850, the  $K_{ML}$  that gives the best agreement between the calculated and observed absorbances was determined. While the absorbance maxima of the *rac*-EHPG complex is constant at 480 nm throughout the p[H] range shown, the *meso*-EHPG complex reveals a shift from 485 nm to slightly higher wavelengths as the p[H] is lowered. This shift corresponds to formation of the protonated metal chelate species MHL revealed in the potentiometric data analysis. In the case of the [Fe(*meso*-EHPG)]<sup>-</sup> there

(31) Sundberg, R. J.; Martin, R. B. *Chem. Rev.* 1974, 74, 481.



**Figure 7.** Species distributions vs  $p[H]$  of 1:1 In(III)/*meso*-EHPG (left) and 1:1 In(III)/*rac*-EHPG (right). Temperature, 25.0 °C;  $\mu = 0.10$  M (KCl); concentration of In(III) and ligands,  $1.00 \times 10^{-3}$  M.

is sufficient free metal ion at  $p[H]$  2 in order to get a handle on the constant. However, inspection of the best fit analysis of the potentiometric data revealed that even at  $p[H]$  2 the solubility product of  $Fe(OH)_3$  had been exceeded. Since the possible presence of small amounts of precipitate are masked by the intense absorbance of the Fe(III) complex, it was decided that this formation constant could more reliably be determined spectrophotometrically.

While the affinities of both ligands for Ga(III) and Fe(III) could be expected to be similar based upon consideration of the ionic radii of the two metal ions [Fe(III), 0.785 Å; Ga(III), 0.76 Å<sup>32</sup>], the fact that the Fe(III) complexes have higher stability constants than their corresponding Ga(III) complexes may be a reflection of the greater covalent character of the Fe(III) coordinate bonds to EHPG. Somewhat more surprising was how significantly the increased size of In(III), 0.94 Å,<sup>32</sup> affects the stabilities of the complexes. The approximately 24% increase in atomic radius results in a decrease in stability from the corresponding Ga(III) complexes of some 7 orders of magnitude. The  $p[H]$  profiles, shown in Figure 3, for the [1:1] metal:ligand systems of both ligands are quite different. The racemic EHPG complex shows a break at  $a$  values of 2 and 4, while with the *meso* isomer the breaks occur at  $a$  values of 3 and 4. The species distribution curves shown in Figure 7 provide an illustration of the succession of complexes formed by each ligand with In(III). One will note for the racemic ligand that  $InHL^-$  is never a dominant metal complex species. Apparently the racemic ligand prefers a tetra-coordinate complex at low  $p[H]$ , which presumably excludes both phenolate donor groups. It is likely that this complex has a *cis-α* arrangement analogous to that of EDDA (*N,N'*-ethylenediaminediacetic acid).<sup>33</sup> As the  $p[H]$  is increased, the phenols are deprotonated almost simultaneously as the complex forms the hexacoordinate structure **B** shown in Figure 4. On the other hand, the protonations of the *meso* isomer complex occur stepwise as seen for the divalent metal ions. Presumably the first protonation occurs on the axially coordinated phenolate oxygen (Figure 4), resulting in a stable pentacoordinate complex that, unlikely its racemic ligand counterpart, is dominant in the  $p[H]$  range from approximately 3.5 to 6.0. For the *meso* isomer the tetra-coordinate complex becomes dominant only below  $p[H]$  3.5. Of the trivalent metals, only In(III) shows the presence of diprotonated metal chelates. As the magnitude of the stability constant of the  $ML^-$  species in these trivalent metal ion complexes decreases the importance of the protonated metal complexes increases. This is illustrated by the two extremes of Fe(III), which shows no protonated metal complexes with racemic EHPG, and In(III), which shows a dominant diprotonated metal complex at

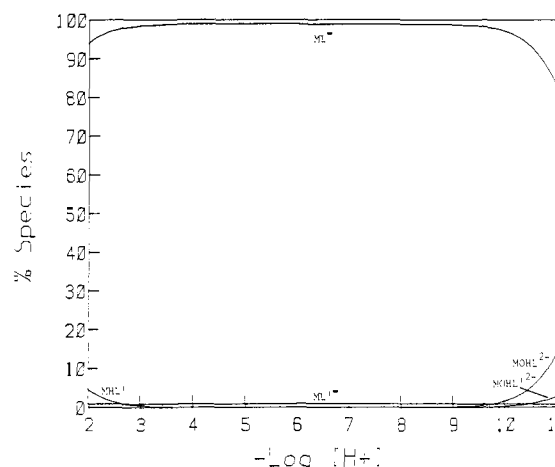


**Figure 8.** Species distribution vs  $p[H]$  of 1:5:5 Fe(III)/*rac*-EHPG/*meso*-EHPG. Temperature, 25.0 °C;  $\mu = 0.10$  M (KCl); concentration of Fe(III),  $1.00 \times 10^{-6}$  M; concentration of each ligand,  $5.00 \times 10^{-6}$  M; L = *rac*-EHPG; L' = *meso*-EHPG.

low  $p[H]$  with the racemic mixture (Figure 7).

Both ligands reveal the formation of hydroxo metal chelates of Fe(III) and In(III) in the  $p[H]$  region accessible to potentiometric measurements (Table V). In the case of Ga(III) the approach to equilibrium at high  $p[H]$  was extremely slow, possibly due to gallate formation, and an accurate measure of the hydrolysis constants could not be determined from the potentiometric experiments. For the racemic mixture the  $\log K_{GaH_2L}$  value is estimated to be approximately 12.0. Patch et al.<sup>6</sup> measured hydroxo metal chelate formation for both complexes of Fe(III) based on the observed spectral shifts that occur at high  $p[H]$ . While the value determined potentiometrically in this study for the hydrolysis of  $[Fe(meso-EHPG)]^-$  ( $\log K_{MH_2L} = 10.45$ ) is in fairly good agreement with the previously determined value ( $\log K_{MH_2L} = 10.3$ ), there is less agreement between the values determined for the racemic form. The value of  $\log K_{MH_2L} = 12.6$  reported by these authors seems unreasonably high in light of chelate hydrolysis constants determined for Fe(III) complexes of ligands with similar donor groups such as SHBED (*N,N'*-bis(2-hydroxy-5-sulfobenzyl)ethylenediamine *N,N'*-diacetic acid) which had a  $\log K_{MH_2L} = 10.57$ .<sup>34</sup> The octahedral complexes of both forms of Fe(EHPG) are distorted from their ideal geometry,<sup>25</sup> hence one would expect substitution of a hydroxide ion for one

(32) Shannon, R. D. *Acta Crystallogr.* 1976, A32, 751.

(33) Srdanov, G.; Herak, R.; Radanovic, D. J.; Veselinovic, D. S. *Inorg. Chim. Acta* 1980, 38, 37.

(34) Motekaitis, R. J.; Martell, A. E. *Inorg. Chim. Acta*, in press.

(35) Aisen, P.; Liebman, A.; Zweier, J. *J. Biol. Chem.* 1978, 253, 1930.

(36) Harris, W. R.; Pecoraro, V. L. *Biochemistry* 1983, 22, 292.

**Table VI.** pM Values and Species Present in the Competition between Transferrin and EHPG for Trivalent Metal Ions ( $[M^{3+}] = 1.0 \times 10^{-6}$  M;  $[Tran] = [EHPG] = 1.0 \times 10^{-5}$  M;  $p[H] 7.4$ )

ligand	pM	concn, %						
		MTran	M <sub>2</sub> Tran	ML	MHL	MH <sub>2</sub> L	MOHL	M(OH) <sub>4</sub> <sup>-</sup>
Metal Ion, Fe(III) <sup>a</sup>								
<i>rac</i> -EHPG	26.9	0	0	100.0			0	
<i>meso</i> -EHPG	24.9	0.1	0	99.8	0		0.1	
Metal Ion, Ga(III) <sup>a</sup>								
<i>rac</i> -EHPG	25.3	0	0	100.0	0			0
<i>meso</i> -EHPG	24.0	0.4	0	99.6	0			0
Metal Ion, In(III) <sup>a</sup>								
<i>rac</i> -EHPG	18.1	97.5	0	2.5	0	0	0	
<i>meso</i> -EHPG	16.9	99.8	0	0.2	0	0	0	

<sup>a</sup>The complex constants  $\log K^*_{ML}$ ,  $\log K^*_{M_2L}$ , and  $[HCO_3^-]$  were, respectively, as follows: Fe(III)-transferrin, 20.67, 19.38,  $1.4 \times 10^{-4}$  M<sup>35</sup>; Ga(III)-transferrin, 20.3, 19.3,  $5.0 \times 10^{-3}$  M<sup>36</sup>; In(III)-transferrin (est) 18.8, 17.9,  $1.4 \times 10^{-4}$  M.

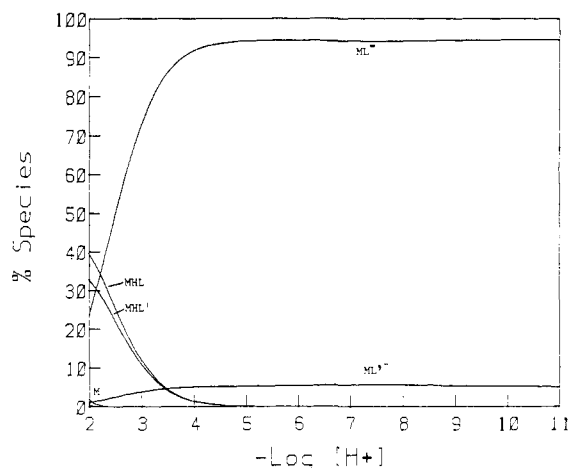


**Figure 9.** Species distribution vs p[H] of 1:5:5 Ga(III)/*rac*-EHPG/*meso*-EHPG. Temperature, 25.0 °C;  $\mu = 0.10$  M (KCl); concentration of Ga(III),  $1.00 \times 10^{-6}$  M; concentration of each ligand,  $5.00 \times 10^{-6}$  M; L = *rac*-EHPG; L' = *meso*-EHPG.

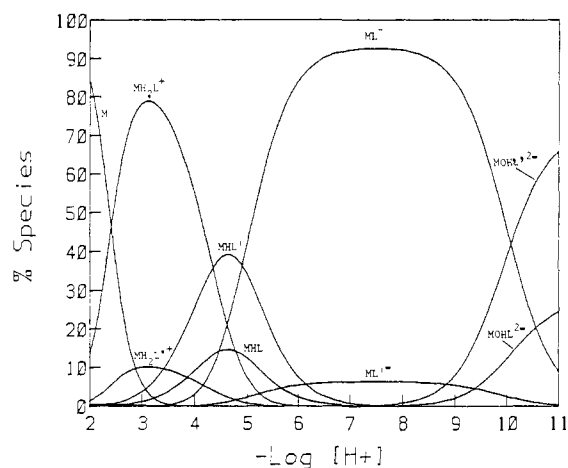


**Figure 10.** Species distribution vs p[H] of 1:5:5 In(III)/*rac*-EHPG/*meso*-EHPG. Temperature, 25.0 °C;  $\mu = 0.10$  M (KCl); concentration of In(III),  $1.00 \times 10^{-6}$  M; concentration of each ligand,  $5.00 \times 10^{-6}$  M; L = *rac*-EHPG; L' = *meso*-EHPG.

of the carboxylate groups to occur well below p[H] 12.6.

In Figures 8–10 are shown species distribution curves for systems containing both the racemic and meso forms of EHPG with a total ligand to metal ratio of 10:1. Both the Fe(III) and Ga(III) systems reveal that the metal ion prefers to distribute itself to the racemic form of EHPG throughout the p[H] range from 2 to 11. When a ligand is used as a radiopharmaceutical carrier of <sup>68</sup>Ga(III) and <sup>111</sup>In(III) in positron emission tomography, it is routinely used in 10-fold or greater excess to assure that all of the metal ion is complexed. If a commercial mixture of both forms

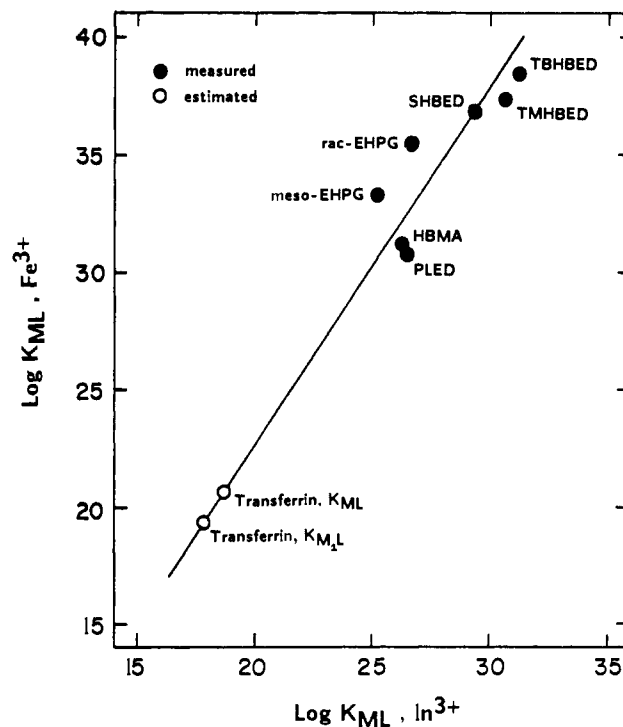


**Figure 11.** Correlation diagram of log stability constants for a series of Fe(III) and In(III) complexes. Temperature, 25.0 °C;  $\mu = 0.10$  M. Values for *rac*- and *meso*-EHPG from Table IV. Fe-transferrin values from ref 35. In-transferrin values estimated. Other values from ref 34. SHBED, *N,N'*-bis(2-hydroxy-5-sulfobenzyl)ethylenediamine-*N,N'*-diacetic acid; TBHBED, *N,N'*-bis(5-*tert*-butyl-2-hydroxy-3-methylbenzyl)ethylenediamine-*N,N'*-diacetic acid; TMHBED, *N,N'*-bis(2-hydroxy-3,5-dimethylbenzyl)ethylenediamine-*N,N'*-diacetic acid; HBMA, *N,N'*-bis(2-hydroxy-3,5-dimethylbenzyl)ethylenediamine-*N*-(2-hydroxyethyl)-*N'*-acetic acid; PLED, *N,N'*-bis(pyridoxyl)ethylenediamine-*N,N'*-diacetic acid.

of EHPG (~50–50) were used in 10-fold excess to prepare complexes of <sup>68</sup>Ga(III) and <sup>111</sup>In(III) at a physiological p[H] of 7.4, the behavior of such a sample in vitro would closely follow that of the racemic form alone. It should be noted though that in the case of In(III) the complexes of the *rac*-EHPG are not always dominant. In fact the distribution of In(III) between the two forms of the ligand is significantly dependent upon the p[H]. Only below p[H] 2.7 and between p[H] 6.2–8.8 are the meso isomer complexes less than 10% of the total metal complex species. Outside of these p[H] ranges the *meso*-EHPG complexes make varying but significant contributions to the distribution of In(III) and in fact become the dominant solution species beyond p[H] 10.3.

In order to compare the total ion sequestering ability of both racemic and meso forms of EHPG with the iron transport protein transferrin it is necessary to calculate pM values, where  $pM = -\log [M]$  and  $[M]$  is the concentration of the free aquo metal ion.

The relative order of the  $pM$  values given in Table VI holds only for the conditions specified: 1  $\mu\text{M}$  metal ion, 10  $\mu\text{M}$  ligand, and  $p[\text{H}]$  7.4. Under a different set of conditions the  $pM$  values would change and even the relative order could vary. As the value of  $pM$  increases so does the affinity of the ligand for the metal ion under the conditions specified. Table VI also provides a comparison of the distribution of metal ion between transferrin and both forms of EHPG for the trivalent metal ions Fe(III), Ga(III), and In(III). Since the stability constants for In(III)-transferrin complexes have not been measured, the correlation between  $\log K_{\text{ML}}$  values for a series of ligands with Fe(III) and In(III) was used to arrive at a reasonable estimate of  $\log K_{\text{ML}}^*$  and  $\log K_{\text{M}_2\text{L}}^*$  for In(III)-transferrin (Figure 11). The series of ligands chosen all contain phenolate (pyridinololate in the case of PLED), amino, and carboxylate donor groups analogous to those found in the active site of transferrin. The values of  $\log K_{\text{ML}}^*$  and  $\log K_{\text{M}_2\text{L}}^*$

estimated for In(III)-transferrin are 18.8 and 17.9, respectively, at 25.0  $^\circ\text{C}$ ,  $\mu = 0.10$  M, and  $[\text{HCO}_3^-] = 1.4 \times 10^{-4}$  M. While the results in Table VI indicate that both EHPG complexes of Fe(III) and Ga(III) would be thermodynamically stable in the presence of transferrin, this is not the case for the In(III) complexes. Now whether these thermodynamically unfavorable reactions will also be sufficiently kinetically unfavorable to make the In-EHPG complexes less useful as radiopharmaceuticals will require additional kinetic studies.

**Acknowledgment.** This research was supported in part by Grant No. CA-42925 from the National Institutes of Health and by a grant from the Texas A&M Institute for Biosciences and Technology. C.J.B. wishes to thank the Robert A. Welch Foundation for a Predoctoral Fellowship. We also express our thanks to Ramunas Motekaitis for computational assistance.

## Synthesis, Structure, and Bonding of Mononuclear Aryloxo Derivatives of Niobium in Oxidation States +5, +3, +2, and +1

Timothy W. Coffindaffer,<sup>†</sup> Bryan D. Steffy,<sup>†</sup> Ian P. Rothwell,<sup>\*,†,1</sup> Kirsten Folting,<sup>†</sup> John C. Huffman,<sup>†</sup> and William E. Streib<sup>†</sup>

Contribution from the Department of Chemistry, Purdue University, West Lafayette, Indiana 47907, and Molecular Structure Center, Indiana University, Bloomington, Indiana 47405. Received August 5, 1988

**Abstract:** The reduction of a series of niobium(V) aryloxides in the presence of the chelating phosphine dmpe ( $\text{dmpe} = \text{Me}_2\text{PCH}_2\text{CH}_2\text{PMe}_2$ ) has been investigated. Treatment of hydrocarbon solutions of either  $\text{Nb}_2(\text{OAr-4Me})_{10}$  (**1a**) or  $\text{Nb}_2(\text{OAr-3,5Me}_2)_{10}$  (**1b**) ( $\text{OAr-4Me} = 4\text{-methylphenoxide}$ ;  $\text{OAr-3,5Me}_2 = 3,5\text{-dimethylphenoxide}$ ) with sodium/amalgam (3 equiv) in the presence of dmpe (2 equiv) leads to the deep purple species  $\text{Nb}(\text{OAr-4Me})_2(\text{dmpe})_2$  (**2a**) and  $\text{Nb}(\text{OAr-3,5Me}_2)_2(\text{dmpe})_2$  (**2b**), respectively. Spectroscopic and magnetic data on these compounds is consistent with them containing low spin  $d^3$ -configurations, while a solid-state structure of **2a** shows a pseudooctahedral environment about the niobium atom with mutually *trans*-aryloxo ligands. Treatment of **2b** with  $\text{HOAr-3,5Me}_2$  (2 equiv) is found to lead to oxidation and the formation of a mixed-valence salt of composition  $[\text{Nb}(\text{OAr-3,5Me}_2)_2(\text{dmpe})_2]^+ [\text{Nb}(\text{OAr-3,5Me}_2)_6]^-$  (**3b**). Treatment of  $\text{Nb}_2(\text{OAr-3,5Me}_2)_{10}$  with Na/Hg (1 equiv) in the presence of dmpe was also found to yield **3b**. The  $^1\text{H}$  NMR of **3b** clearly show the noncontact shifted spectra for the low spin  $d^2$ -cation and  $d^0$ -anion. A solid-state study of **3b** confirmed the formulation and showed the monocation to contain *trans*-aryloxides as in the neutral **2a**. However, differences in the orientations of the aryloxo aryl rings within **2a** and **3b** were noted. The treatment of **2b** with CO (1 atm) was found to lead to the 18-electron dicarbonyl  $\text{Nb}(\text{OAr-3,5Me}_2)(\text{CO})_2(\text{dmpe})_2$  (**4b**). A monocapped, trigonal-prismatic structure for **4b** was found in the solid state with the aryloxo ligand being the capping group. A small angle of only 66.7 ( $^\circ$ ) was also found to exist between the two carbonyl groups in **4b**. The structural parameters in all of these molecules and in particular the Nb-OAr bond lengths and angles have been evaluated and discussed in terms of the importance of oxygen-p to metal-d  $\pi$ -bonding. In this context the solid-state (trigonal-bipyramidal) structure of the monomeric niobium(V) aryloxo  $\text{Nb}(\text{OAr-2,6Me}_2)_5$  (**1c**) has also been determined for comparison. The summary of the crystal data is as follows: for  $\text{Nb}(\text{OAr-2,6Me}_2)_5$  (**1c**) at 24  $^\circ\text{C}$ ,  $a = 11.854$  (6)  $\text{\AA}$ ,  $b = 16.305$  (4)  $\text{\AA}$ ,  $c = 18.140$  (5)  $\text{\AA}$ ,  $\beta = 99.44$  ( $^\circ$ ),  $Z = 4$ ,  $d_{\text{calcd}} = 1.312$   $\text{g cm}^{-3}$  in space group  $P2_1/n$ ; for  $\text{Nb}(\text{OAr-4Me})_2(\text{dmpe})_2$  (**2a**) at -158  $^\circ\text{C}$ ,  $a = 12.646$  (4)  $\text{\AA}$ ,  $b = 14.016$  (5)  $\text{\AA}$ ,  $c = 9.707$  (3)  $\text{\AA}$ ,  $\alpha = 110.87$  ( $^\circ$ ),  $\beta = 105.83$  ( $^\circ$ ),  $\gamma = 76.21$  ( $^\circ$ ),  $Z = 2$ ,  $d_{\text{calcd}} = 1.321$   $\text{g cm}^{-3}$  in space group  $P1$ ; for  $[\text{Nb}(\text{OAr-3,5Me}_2)_2(\text{dmpe})_2][\text{Nb}(\text{OAr-3,5Me}_2)_6]$  (**3b**) at -156  $^\circ\text{C}$ ,  $a = 27.96$  (2)  $\text{\AA}$ ,  $b = 23.49$  (2)  $\text{\AA}$ ,  $c = 13.32$  (1)  $\text{\AA}$ ,  $\beta = 119.72$  ( $^\circ$ ),  $Z = 4$ ,  $d_{\text{calcd}} = 1.272$   $\text{g cm}^{-3}$  in space group  $P2_1/a$ ; for  $\text{Nb}(\text{OAr-3,5Me}_2)(\text{CO})_2(\text{dmpe})_2$  (**4b**) at -160  $^\circ\text{C}$ ,  $a = 16.751$  (3)  $\text{\AA}$ ,  $b = 12.133$  (2)  $\text{\AA}$ ,  $c = 27.331$  (7)  $\text{\AA}$ ,  $Z = 8$ ,  $d_{\text{calcd}} = 1.364$   $\text{g cm}^{-3}$  in space group  $Pcab$ .

The last few years have seen a dramatic increase in research interest into the chemistry of the heavier group 5 elements (Nb, Ta) in their lower oxidation states. This interest has been prompted by the demonstrated high reactivity exhibited by low-valent niobium and tantalum complexes.<sup>2-10</sup> Activation of  $\text{N}_2$ , CO, acetylenes, and  $\text{H}_2$  as well as the cleavage of CH bonds have all been associated with these types of complexes. Furthermore, the possibility for the formation of reactive metal-metal multiple bonds that are either novel or complimentary to their widely

studied group 6 metal neighbors has further increased this interest.<sup>3,4,9,10</sup> Typical synthetic strategies have involved the reduction

(1) Camille and Henry Dreyfus Teacher-Scholar, 1985-1990. Fellow of the Alfred P. Sloan Foundation, 1986-1990.

(2) (a) Dewey, C. G.; Ellis, J. E.; Fjane, K. L.; Fahl, K. M. P.; Warrock, G. F. P. *Organometallics* **1983**, *2*, 388. (b) Warrock, G. F. P.; Ellis, J. E. *J. Am. Chem. Soc.* **1984**, *106*, 5016.

(3) (a) Cotton, F. A.; Falvello, L. R.; Najaar, R. C. *Inorg. Chem.* **1983**, *22*, 375. (b) Cotton, F. A.; Roth, W. J. *Inorg. Chem.* **1983**, *22*, 868. (c) Cotton, F. A.; Roth, W. J. *Inorg. Chem.* **1984**, *23*, 845. (d) Cotton, F. A.; Roth, W. J. *J. Am. Chem. Soc.* **1983**, *105*, 3734. (d) Cotton, F. A.; Roth, W. J. *J. Am. Chem. Soc.* **1984**, *106*, 4749.

<sup>†</sup>Purdue University.

<sup>†</sup>Indiana University.